Decoherence of a superconducting qubit due to bias noise

John M. Martinis, S. Nam, J. Aumentado, and K. M. Lang*
National Institute of Standards and Technology, 325 Broadway, Boulder, Colorado 80305-3328

C. Urbina†
Service de Physique de l'Etat Condens, Commissariat l'Energie Atomique, Saclay, F-91191 Gif-sur-Yvette Cedex, France
(Received 26 September 2002; published 25 March 2003)

We calculate for the current-biased Josephson junction the decoherence of the qubit state from noise and dissipation. The effect of dissipation can be entirely accounted for through a semiclassical noise model that appropriately includes the effect of zero-point and thermal fluctuations from dissipation. The magnitude and frequency dependence of this dissipation can be fully evaluated with this model to obtain design constraints for small decoherence. We also calculate decoherence from spin echo and Rabi control sequences and show they are much less sensitive to low-frequency noise than for a Ramsey sequence. We predict small decoherence rates from $1/f$ noise of charge, critical current, and flux based on noise measurements in prior experiments. Our results indicate this system is a good candidate for a solid-state quantum computer.

DOI: 10.1103/PhysRevB.67.094510 PACS number(s): 03.65.Yz, 03.67.Lx, 85.25.Cp

I. INTRODUCTION

The potential to manipulate information efficiently with quantum mechanics[1] has led to a search for a physical system that could implement a quantum computer scalable to large size. Superconducting circuits are favorable candidates[2] because the nonlinearity of Josephson junctions can be used to construct two-level quantum systems (qubits), the inherently low dissipation of superconductors make possible long coherence times, and integrated circuit technology allows scaling to large and complex circuits.

Recently, several experiments have demonstrated the potential of superconducting qubits with the observation of Rabi oscillations,[3,4] long coherence times,[5,6] and high-fidelity state preparation and measurement.[7] Future experiments need to improve these results, as well as demonstrate logic operations by coupling the qubits via circuit elements such as inductors, capacitors, and wires.

The same wires that make these ''superconducting atoms'' easy to manipulate, measure, and scale unfortunately also couple the qubit to other electromagnetic degrees of freedom that can be a source of decoherence via dissipation and noise. A significant experimental challenge is to understand how to design these wires, balancing the competing demands for coupling and coherence.

Such a balance requires a detailed theoretical understanding of mechanisms of decoherence. The main purpose of this paper is to give a physical picture of decoherence, showing that it can be understood as a random fluctuation in the qubit state arising from noise.

The amount of decoherence may be calculated from the spectral density of the total noise of the current bias. We consider spectral densities for an arbitrary source and bias impedance, as well as $1/f$ noise from fluctuations in critical current, charge, and flux. The frequency dependence of the spectral density affects the time dependence of decoherence. For $1/f$ spectral densities, this dependence may be exploited to greatly reduce decoherence by properly choosing the time sequence of the qubit manipulation.

The outline of the paper is as follows. In Sec. II we reexpress the Hamiltonian of the current-biased Josephson junction system as an effective two-state Hamiltonian that allows full manipulation of the qubit state via the control currents. In Sec. III, noise in these control currents is shown to fluctuate the state of the qubit. These fluctuations cause the measurement of the qubit state to deviate from the expected value and are equivalent to decoherence. We show in Sec. IV that these fluctuations can arise from the finite impedance of the current bias and can be accounted for semiclassically with quantum noise. Resistive (frequency independent) dissipation is then considered and used to place limits on the magnitude of the current-bias impedance. In Sec. 28 we calculate how an arbitrary resonance affects decoherence. This result can be used to estimate decoherence for a current bias that has frequency-dependent dissipation. Because this noise model readily predicts decoherence for an arbitrary noise spectral density and state sequence of the qubit, we calculate in Sec. VI decoherence for spin echo and Rabi sequences. We argue that these sequences should be used for quantum computation because they are insensitive to low frequency $1/f$ noise. Experimental values of $1/f$ noise are then used to estimate decoherence rates for the current-biased Josephson junction. In Sec. VII we show that decoherence differs qualitatively for Gaussian and non-Gaussian noise sources, and that decoherence from the latter can mimic a loss in measurement fidelity.

Although some of these results are identical to that found in previous theoretical work for Josephson systems using environmental and spin-boson models,[9,2,8,10,11] we believe this paper is especially useful because the noise model gives a more physical description to the origins of the decoherence and can thus be generalized readily to more complex experimental situations. Since the performance of electronic systems is typically evaluated using noise models and noise can be classically understood and measured, we believe this approach will be a particularly insightful for the Josephson, and indeed many other qubit systems.

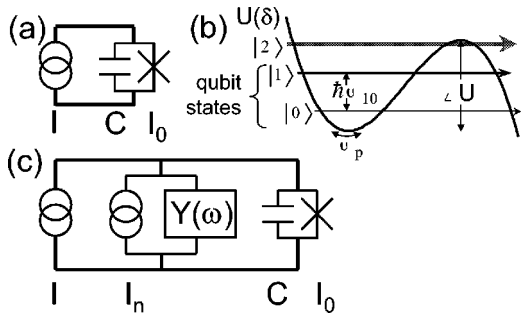

FIG. 1. (a) Model of a current-biased Josephson junction without dissipation (infinite impedance of current bias). (b) Cubic potential U showing qubit states. (c) Circuit model including finite impedance current bias, represented by admittance Y and its noise I_n.

II. THE CURRENT-BIASED JOSEPHSON JUNCTION

In this section we describe the basic physics of the current-biased Josephson junction, showing that when its two lowest energy levels are used as a qubit, the qubit state can be fully manipulated with low- and microwave-frequency control currents. In a Bloch sphere description of the state, we show that these control currents simply rotate the Bloch vector. We consider here a circuit model without dissipation, as shown in Fig. 1(a), whereas the full model with dissipation [Fig. 1(c)] is considered later in Sec. IV.

The quantum behavior of the current-biased Josephson junction has been described in detail elsewhere.[12–14] The Hamiltonian of the system of Fig. 1(a) with bias source I, junction critical current I_0, and junction capacitance C is

$$H=\frac{1}{2C}\hat{Q}^2-\frac{I_0\Phi_0}{2\pi}\cos\hat{\delta}-\frac{I\Phi_0}{2\pi}\hat{\delta}, \tag{1}$$

where $\Phi_0=h/2e$ is the superconducting flux quantum. The operators $\hat{Q}$ and $\hat{\delta}$ correspond to the charge and the superconducting phase difference across the junction, respectively, and have a commutation relationship $[\hat{\delta},\hat{Q}]=2ei$. Quantum mechanical behavior can be observed for large area junctions in which $I_0\Phi_0/2\pi=E_J\gg E_C=e^2/2C$ when the bias current is slightly smaller than the critical current $I\lesssim I_0$. In this regime the last two terms in H can be accurately approximated by a cubic potential $U(\delta)$ parametrized by a barrier height $\Delta U(I)=(2\sqrt{2}I_0\Phi_0/3\pi)[1-I/I_0]^{3/2}$ and a quadratic curvature at the bottom of the well that gives a classical oscillation frequency $\omega_p(I)=2^{1/4}(2\pi I_0/\Phi_0 C)^{1/2}[1-I/I_0]^{1/4}$ [see Fig. 1(b)]. This plasma frequency can be understood as the junction resonance frequency $\omega_p=1/\sqrt{L_JC}$, where the Josephson inductance is $L_J=\Phi_0/2\pi I_0\cos\delta_a$ and the average phase δ_a is given through $I=I_0\sin\delta_a$. It is useful to think of this system as an anharmonic "LC" oscillator created from the Josephson inductance and the junction capacitance, with the anharmonicity arising from the nonlinear $1/\cos\delta$ term in L_J.

The commutation relation leads to quantized energy levels in the cubic potential,[15] with the two lowest levels being used as the qubit states. Microwaves induce transitions between levels at a frequency $\omega_{mn}=E_{mn}/\hbar=(E_m-E_n)/\hbar$, where E_n is the energy of state $|n\rangle$. The two lowest transitions have frequencies

$$\omega_{10}\simeq\omega_p\left(1-\frac{5}{36}\frac{\hbar\omega_p}{\Delta U}\right) \tag{2a}$$

and

$$\omega_{21}\simeq\omega_p\left(1-\frac{5}{18}\frac{\hbar\omega_p}{\Delta U}\right). \tag{2b}$$

These two frequencies must be different for the qubit to behave as a two-state system. The ratio $\Delta U/\hbar\omega_p$ parametrizes the anharmonicity of the cubic potential with regards to the qubit states. Because typical operation selects the number of states in the well to be approximately $\Delta U/\hbar\omega_p\sim 4$, the transition frequency between qubit states is $\omega_{10}\simeq 0.96\omega_p$ and the separation of the two lowest resonant frequencies is $\omega_{10}-\omega_{21}\simeq 0.034\omega_{10}$.

The state of the qubit can be controlled with the bias current, which may be written as

$$I(t)=I_{dc}+\Delta I(t) \tag{3a}$$

$$=I_{dc}+I_{lf}(t)+I_{\mu wc}(t)\cos\omega_{10}t+I_{\mu ws}(t)\sin\omega_{10}t. \tag{3b}$$

We require that the currents I_{lf}, $I_{\mu wc}$, and $I_{\mu ws}$ are varied in time slowly compared to $2\pi/(\omega_{10}-\omega_{21})\sim 3$ ns to inhibit $1\rightarrow 2$ transitions. These long pulses restrict the dynamics of the system to the Hilbert space spanned by the lowest two states. The Hamiltonian for *only* these two states is

$$H_2=\begin{pmatrix} E_0+\langle 0|\hat{\delta}|0\rangle\frac{\Phi_0}{2\pi}\Delta I & \langle 0|\hat{\delta}|1\rangle\frac{\Phi_0}{2\pi}\Delta I \\ \langle 1|\hat{\delta}|0\rangle\frac{\Phi_0}{2\pi}\Delta I & E_1+\langle 1|\hat{\delta}|1\rangle\frac{\Phi_0}{2\pi}\Delta I \end{pmatrix}, \tag{4}$$

where the full Hamiltonian is solved for $I=I_{dc}$ to obtain the basis states $|0\rangle$ and $|1\rangle$ and corresponding eigenenergies E_0 and E_1.

The off-diagonal matrix elements are well approximated by the harmonic oscillator value $\langle 0|\hat{\delta}|1\rangle=(2\pi/\Phi_0)\sqrt{\hbar/2\omega_{10}C}$ due to the small nonlinearity of this system. By removing nonresonant terms and reexpressing the Hamiltonian H_2 in the ω_{10} rotating frame where $\exp(-i\omega_{10}t)|1\rangle\rightarrow|1\rangle$, we find

$$\begin{aligned} H_{(2)}=&\hat{\sigma}_x I_{\mu wc}(t)\sqrt{\hbar/2\omega_{10}C}/2, \\ &+\hat{\sigma}_y I_{\mu ws}(t)\sqrt{\hbar/2\omega_{10}C}/2, \\ &+\hat{\sigma}_z I_{lf}(t)(\partial E_{10}/\partial I_{dc})/2, \end{aligned} \tag{5}$$

where $\hat{\sigma}_{x,y,z}$ are Pauli operators.

The form of $H_{(2)}$ implies that the qubit state can be fully manipulated with the classical bias currents $I_{\mu wc}(t)$, $I_{\mu ws}(t)$,

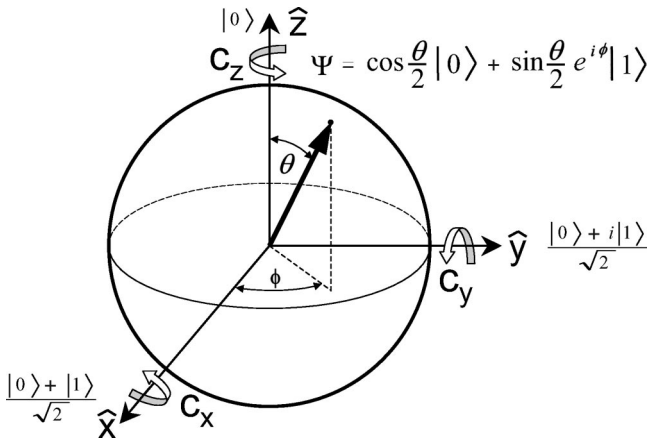

FIG. 2. Bloch sphere representation of the qubit state. Control vector $c=(c_x,c_y,c_z)$ rotates the Bloch vector around axis of direction $c_x\hat{x}+c_y\hat{y}+c_z\hat{z}$ with angle $|c|$.

and $I_{lf}(t)$. If these control currents have constant values over time Δt, we can define a control vector $\vec{c}=(c_x,c_y,c_z)$ with

$$\vec{c}=\left(I_{\mu wc}\sqrt{\frac{\hbar}{2\omega_{10}C}},I_{\mu ws}\sqrt{\frac{\hbar}{2\omega_{10}C}},I_{lf}\frac{\partial E_{10}}{\partial I_{dc}}\right)\frac{\Delta t}{\hbar}. \quad (6)$$

The control currents change the qubit state after time Δt according to the unitary transformation[1]

$$U=\exp[-iH_{(2)}\Delta t/\hbar], \quad (7a)$$

$$=\exp[-i\hat{\sigma}\cdot\vec{c}/2], \quad (7b)$$

$$=\hat{\sigma}_0\cos\frac{|\vec{c}|}{2}-i\frac{\hat{\sigma}\cdot\vec{c}}{|\vec{c}|}\sin\frac{|\vec{c}|}{2}, \quad (7c)$$

where $\hat{\sigma}=(\hat{\sigma}_x,\hat{\sigma}_y,\hat{\sigma}_z)$ and $\hat{\sigma}_0$ is the identity matrix.

One way to visualize how $\vec{c}$ controls the qubit state is via the standard Bloch-sphere description. As illustrated in Fig. 2, the direction of the Bloch vector describes the qubit state according to $\Psi=\cos(\theta/2)|0\rangle+\sin(\theta/2)\exp(i\phi)|1\rangle$. The angle θ of the vector corresponds to the occupation amplitude of the state, whereas the angle ϕ gives the phase of the state. The probability of measuring the ground state is given by $\cos^2(\theta/2)$. Operations of $\hat{\sigma}_x$, $\hat{\sigma}_y$, and $\hat{\sigma}_z$ correspond to rotations of the state vector around the $\hat{x}$, $\hat{y}$, and $\hat{z}$ axis, respectively. In general, a control vector $\vec{c}$ rotates the Bloch vector around the $\vec{c}$ axis with angle $|\vec{c}|$. For example, a "$\pi/2$-pulse" with control vector $\vec{c}=(0,\pi/2,0)$ changes the state $|0\rangle$ to the state $(|0\rangle+|1\rangle)/\sqrt{2}$.

III. CALCULATION OF DECOHERENCE FOR AN ARBITRARY NOISE SOURCE

Because the bias current controls the qubit, noise in the bias current fluctuates the qubit state and causes decoherence. In this section we calculate how noise randomly rotates the Bloch vector around the three axes. Because we separated the effect of the bias current into low $I_{lf}(t)$ and microwave frequency $I_{\mu wc}(t)\cos\omega_{10}t+I_{\mu ws}(t)\sin\omega_{10}t$ components, the effect of noise can be separated likewise. Since the net effect of these rotations depends on the state of the qubit, we calculate how these fluctuations affect the measurement of the state for two typical experimental situations.

Current noise at low frequency fluctuates the c_z component of the control vector, which randomly rotates the Bloch vector around the $\hat{z}$ axis due to $\hat{\sigma}_z$ operations. These random rotations produce noise in the phase ϕ of the qubit state. Since the phase is $\phi(t)=\int_0^t dt\,\omega_{10}(t)$, the phase noise after a time t is

$$\phi_n(t)=\frac{\partial\omega_{10}}{\partial I_{dc}}\int_0^t dt' I_n(t'). \quad (8)$$

Physically, phase noise arises from noise current flowing through the nonlinear inductance of the junction that in turn causes ω_{10} to vary.

The magnitude of the phase noise is described by its mean-squared value $\langle\phi_n^2(t)\rangle$. This quantity is calculated with the noise power of I_n, described as the spectral density $S_I(f)$. It is defined as the mean-squared amplitude of the current noise at frequency f per 1 Hz bandwidth. The time average of the correlation function is computed with the noise power by

$$\langle I_n(t)I_n(0)\rangle=\int_0^\infty df\,S_I(f)\cos 2\pi ft. \quad (9)$$

Using Eq. (8) the mean-squared phase noise is

$$\langle\phi_n^2(t)\rangle=\left(\frac{\partial\omega_{10}}{\partial I_{dc}}\right)^2\left\langle\int_0^t dt' I_n(t')\int_0^t dt'' I_n(t'')\right\rangle \quad (10a)$$

$$=\left(\frac{\partial\omega_{10}}{\partial I_{dc}}\right)^2\int_0^\infty df\,S_I(f)\int_0^t dt'\int_0^t dt''\mathrm{Re}\,e^{i2\pi f(t'-t'')} \quad (10b)$$

$$=\left(\frac{\partial\omega_{10}}{\partial I_{dc}}\right)^2\int_0^{\omega_{10}/2\pi} df\,S_I(f)\,W_0(f), \quad (10c)$$

where $W_0(f)$ is a spectral weight function given by

$$W_0(f)=\left|\int_0^t dt' e^{i2\pi ft'}\right|^2 \quad (11a)$$

$$=\frac{\sin^2(\pi ft)}{(\pi f)^2}. \quad (11b)$$

The phase noise integral is cutoff for frequencies greater than $\omega_{10}/2\pi$. For these frequencies, the noise current primarily flows through the junction capacitance, not the junction, and thus does not significantly modulate ω_{10}. Furthermore, noise *at* ω_{10} should not be included because it is accounted for in stimulated transitions, as computed below. Integrating the noise to a cutoff frequency $\omega_{10}/2\pi$ is a good approximation because for most circuit impedances a change in this cutoff frequency only logarithmically affects the phase noise [see Eq. (26)].

The spectral weight $W_0(f)$ is constant for frequency $f \lesssim 1/t$ and decreases as $1/f^2$ at higher frequencies. This implies that the phase noise has a contribution for most noise sources only from low frequencies. For the case when the low frequency noise is constant (white) and equal to S_I^0, Eqs. (10c) and (11b) can be integrated to yield

$$\langle \phi_n^2(t) \rangle = (\partial \omega_{10}/\partial I_{dc})^2 S_I^0 t/2. \tag{12}$$

Noise at high frequency near ω_{10} produces $0 \rightarrow 1$ and $1 \rightarrow 0$ transitions. The decoherence from these transitions may be calculated in a similar fashion as phase noise. The control current for c_x and c_y is given by $I_{\mu wc}(t)\cos\omega_{10}t + I_{\mu ws}(t)\sin\omega_{10}t$, which implies that mixing from noise around frequency ω_{10} can be represented by low frequency noise in $I_{\mu wc}(t)$ and $I_{\mu ws}(t)$. With a constant spectral density of current noise immediately around ω_{10}, the spectral densities of $I_{\mu wc}$ and $I_{\mu ws}$ are constant and each equal to $2S_I(\omega_{10}/2\pi)$. This noise produces random $\hat{\sigma}_x$ and $\hat{\sigma}_y$ operations that rotates the Bloch vector around the $\hat{x}$ and $\hat{y}$ axes, defined by angles θ_x and θ_y, respectively. The fluctuations of θ_x and θ_y are calculated exactly as for phase noise. Using Eq. (12) with $S_I^0 \rightarrow 2S_I(\omega_{10}/2\pi)$ and replacing $(\partial\omega_{10}/\partial I_{dc})^2 \rightarrow 1/2\hbar\omega_{10}C$ as implied by Eq. (5), we find

$$\langle \theta_x^2(t) \rangle = \langle \theta_y^2(t) \rangle = (1/2\hbar\omega_{10}C) S_I(\omega_{10}/2\pi) t. \tag{13}$$

The probability distributions of ϕ, θ_x, and θ_y are needed to fully describe the noise in the Bloch vector and to predict measurement probabilities. Since the amplitude of the current-bias noise is typically described by Gaussian statistics, the probability density to find a given value of χ is given by

$$\frac{dp(\chi)}{d\chi} = \frac{\exp(-\chi^2/2\langle\chi^2\rangle)}{\sqrt{2\pi\langle\chi^2\rangle}}, \tag{14}$$

where the rotation angles are $\chi = \phi$, θ_x, or θ_y, and $\langle\chi^2\rangle$ is the mean squared noise that has been previously calculated.

We next calculate how these random rotations in the Bloch vector affect the state of the qubit. Because the Bloch state is represented by *two* variables θ and ϕ, but noise produces rotations around the *three* axes $\hat{x}$, $\hat{y}$, and $\hat{z}$, the effect of noise depends on the direction of the Bloch vector. If a state vector has angle ε with respect to a rotation axis, then rotations about that axis moves the vector a distance proportional to $\sin\varepsilon$. In particular, if the Bloch vector points along one of the axes $\hat{x}$, $\hat{y}$, or $\hat{z}$, then $\varepsilon = 0$ and the noise corresponding to that axis has no effect. Rotations from the two remaining axes may be treated independently to first order when the noise is small.

In a first example, we calculate the effect of noise on the ground state and its measurement. When the qubit is initialized to this state, in the absence of noise $\vec{c} = 0$ and the probability to measure the ground state is fixed at $p_0 = 1$. Because the Bloch vector is parallel to the $\hat{z}$ axis, current-bias noise at low frequency has no effect on the state or the measurement. However, noise near the frequency ω_{10} rotates the Bloch vector in both θ_x and θ_y, moving the system away from the ground state and giving $p_0 < 1$. The average probability p_0 of measuring state $|0\rangle$ is calculated from the usual probability of measuring the ground state $\cos^2(\theta/2) \simeq \cos^2[(\theta_x^2 + \theta_y^2)^{1/2}/2]$, integrating[16] over the Gaussian probability distributions of θ_x and θ_y

$$p_0 = \int_{-\infty}^{\infty} d\theta_x \int_{-\infty}^{\infty} d\theta_y \frac{dp(\theta_x)}{d\theta_x} \frac{dp(\theta_y)}{d\theta_y} \cos^2[(\theta_x^2 + \theta_y^2)^{1/2}/2] \tag{15a}$$

$$\simeq 0.5 + 0.5\exp[-(\langle\theta_x^2(t)\rangle + \langle\theta_y^2(t)\rangle)/2] \tag{15b}$$

$$= 0.5 + 0.5\exp[-(1/2\hbar\omega_{10}C) S_I(\omega_{10}/2\pi) t]. \tag{15c}$$

Equation (15b) implies that the Bloch vector fluctuates by the total magnitude $\langle\theta^2\rangle = \langle\theta_x^2\rangle + \langle\theta_y^2\rangle$. Additionally, the exponential decay of p_0 with time implies that the change of the state can be described by the rate

$$\gamma_s = (1/2\hbar\omega_{10}C) S_I(\omega_{10}/2\pi), \tag{16}$$

which corresponds to the $0 \rightarrow 1$ transition rate for stimulated absorption. There is no contribution from phase noise because low frequency noise can not add energy $\hbar\omega_{10}$ to the qubit to excite a $0 \rightarrow 1$ transition.

When the initial state is $|1\rangle$, an identical calculation finds the $1 \rightarrow 0$ transition rate for stimulated emission to be γ_s, as expected. Because the stimulated emission and absorption rates are equal, the probability of measuring the ground state approaches 1/2 at long times, as given by p_0 in Eq. (15c).

In a second example, we calculate the effect of noise on a superposition state that is created and measured in a "Ramsey fringe" experiment. In this case the qubit will be sensitive to both stimulated transitions and phase noise. The state $(|0\rangle + |1\rangle)/\sqrt{2}$ is first created with a $\pi/2$ pulse, then after time t any change in the state is measured by applying a $-\pi/2$ pulse and performing a state measurement. After the initial pulse, the Bloch vector points in the $\hat{x}$ direction and moves from noise only in ϕ and θ_y. Thus after the final pulse the state deviates from $\theta = 0$ by $\langle\theta^2\rangle \simeq \langle\phi_n^2\rangle + \langle\theta_y^2\rangle$. For a spectral density that is white, the phase noise grows linearly with t [Eq. (12)] and can be described with a rate $\gamma_\phi = (\partial\omega_{10}/\partial I_{dc})^2 S_I^0/4$. In this case the total decoherence rate is given by $\gamma_2 = \gamma_\phi + \gamma_s/2$.

These two examples illustrate that the decoherence rate depends on the state of the qubit. The ground state is affected by fluctuations in θ_x and θ_y, with each contributing $\gamma_s/2$ to the total decoherence rate. The superposition state is affected by noise in ϕ and θ_y, which gives a rate $\gamma_\phi + \gamma_s/2$.

Qualitatively, decoherence can be thought of as the deviation of probability measurements from the ideal intended outcome. From the examples in this section, decoherence can be understood as fluctuations in the Bloch vector induced by noise. Since the measured decoherence rate depends on the state of the qubit, a more fundamental representation of decoherence should directly describe fluctuations in the rotations ϕ, θ_x, and θ_y.

IV. DECOHERENCE FROM DISSIPATION

Calculations in previous sections assumed the circuit model of Fig. 1(a) with an ideal bias-current source of infinite impedance. In an actual experiment, the finite impedance of the bias-current source produces decoherence of the qubit from dissipation and its noise. The bias source may be a complicated electrical circuit with many electromagnetic modes. Because its response is typically linear,[18] we can describe it with a frequency-dependent admittance $Y(\omega)$ as shown in Fig. 1(c).

Quantum fluctuations in the bias current are included by no longer considering the quantity $I_n(t')$ in Eq. (8) as a classical variable, but as an operator. Following the derivation of Ref. 17, the effect of quantum and thermal fluctuations can be taken into account semi-classically with the noise model presented in the last section, but with a noise spectral density of positive and negative frequencies. We calculate transition rates and phase noise, and show that dissipation can be understood as a $1\rightarrow 0$ transition induced by zero-point noise. We also consider the case of resistive dissipation and estimate the coherence time for typical junction parameters.

We first consider the current fluctuations from a single LC resonant mode with no damping. The current-current correlation function for this resonant mode is[17]

$$\langle I(t)I(0)\rangle = \frac{\hbar\omega_0}{2L}(\langle c^\dagger c\rangle e^{+i\omega_0 t} + \langle cc^\dagger\rangle e^{-i\omega_0 t}), \quad (17)$$

where $\omega_0 = 1/\sqrt{LC}$ and $c^\dagger$ and c are the normal creation and annihilation operators. Equation (17) can be rewritten, using the thermal-quantum expectation values $\langle c^\dagger c\rangle = 1/[\exp(\hbar\omega_0/kT)-1]$ and $\langle cc^\dagger\rangle = \langle c^\dagger c\rangle + 1$, as

$$\langle I(t)I(0)\rangle = \frac{\hbar\omega_0}{4L}\{[\coth(+\hbar\omega_0/2kT)+1]e^{+i\omega_0 t} - [\coth(-\hbar\omega_0/2kT)+1]e^{-i\omega_0 t}\}. \quad (18)$$

Note that this correlation function has a different magnitude at the positive and negative frequency. Using the Caldeira-Legget representation of dissipation, the admittance $Y(\omega)$ can be constructed from a bath of harmonic oscillators with a density of oscillation frequencies proportional to $\mathrm{Re}\{Y(\omega)\}$, the real (dissipative) part of the admittance. The spectral density of the current noise is obtained by a Fourier transform of Eq. (18) summed over all the oscillator modes, which gives at positive and negative frequencies[17]

$$S_I^{qu}(\omega/2\pi) = \hbar\omega[\coth(\hbar\omega/2kT)+1]\,\mathrm{Re}\,Y(\omega) \quad (19a)$$

$$= \frac{2\hbar\omega}{1-\exp(-\hbar\omega/kT)}\mathrm{Re}\,Y(\omega). \quad (19b)$$

The spectral density at negative and positive frequencies corresponds to the emission and absorption of photons from the admittance Y, as can be understood by the creation and annihilation operators in Eq. (17). The spectral density at negative frequencies corresponds to the blackbody radiation formula for a dissipative element. The $0\rightarrow 1$ transition rate is proportional to the spectral density of noise at the negative frequency $-\omega_{10}$, whereas the $1\rightarrow 0$ rate is given by noise at the positive frequency ω_{10}. The ratio of these two rates are given by

$$\frac{S_I^{qu}(-\omega/2\pi)}{S_I^{qu}(\omega/2\pi)} = \exp(-\hbar\omega/kT), \quad (20)$$

which obeys detailed balance and thus gives occupation probabilities of the two states with the correct Boltzman factor.

The sum and difference of the spectral densities are

$$S_I^{+}(\omega/2\pi) = S_I^{qu}(\omega/2\pi) + S_I^{qu}(-\omega/2\pi) \quad (21a)$$

$$= 2\hbar\omega\,\mathrm{cotanh}(\hbar\omega/2kT)\,\mathrm{Re}\,Y(\omega) \quad (21b)$$

$$= 4kT\,\mathrm{Re}\,Y(\omega) \qquad (\hbar\omega \ll kT) \quad (21c)$$

and

$$S_I^{-}(\omega/2\pi) = S_I^{qu}(\omega/2\pi) - S_I^{qu}(-\omega/2\pi) \quad (22a)$$

$$= 2\hbar\omega\,\mathrm{Re}\,Y(\omega). \quad (22b)$$

The spectral density $S_I^{+}(\omega/2\pi)$ is the conventional expression for the total thermal and quantum noise, whereas $S_I^{-}(\omega/2\pi)$ is the zero-point noise.

We calculate decoherence differently for fluctuations in θ_x, θ_y, and ϕ. For decoherence in the θ directions, fluctuations in θ change the amplitude of the $|0\rangle$ and $|1\rangle$ states, which implies energy has been exchanged with the environment Y. The $0\rightarrow 1$ and $1\rightarrow 0$ transition rates can be computed with the spectral densities of the negative and positive frequencies using the rate γ_s derived in the last section. The $0\rightarrow 1$ transition rate is proportional to $S_I^{qu}(-\omega_{10}/2\pi)$, whereas the $1\rightarrow 0$ rate is proportional to $S_I^{qu}(\omega_{10}/2\pi) = S_I^{qu}(-\omega_{10}/2\pi) + S_I^{-}(\omega/2\pi)$. We can reexpress the effect of both of these rates with two new rates: a decoherence rate $\gamma_{\mathrm{th}} \propto S_I^{qu}(-\omega_{10}/2\pi)$ arising from thermal noise that is *independent* of the transition direction, and a $1\rightarrow 0$ decay rate $\gamma_1 \propto S_I^{-}(\omega/2\pi)$ arising from zero-point noise that corresponds to dissipation. Replacing S_I in Eq. (16) with $S_I^{qu}(-\omega_{10}/2\pi)$ and $S_I^{-}(\omega_{10}/2\pi)$, we find a decoherence rate

$$\gamma_{\mathrm{th}} = \frac{\mathrm{Re}\,Y(\omega_{10})/C}{\exp(\hbar\omega_{10}/kT)-1} \quad (23)$$

and a decay rate

$$\gamma_1 = \mathrm{Re}\,Y(\omega_{10})/C. \quad (24)$$

The decay rate γ_1 agrees with a conventional calculation of spontaneous decay of the $|1\rangle$ state.[19] The thermal decoherence rate γ_{th} is usually negligible because experiments typically operate at low temperature $T \ll \hbar\omega_{10}/k$.

For decoherence in ϕ, no net energy is exchanged with the environment because θ is constant. With no dependence

TABLE I. Typical experimental parameters for a junction of area A that is used in this paper for numerical calculations. Left column lists junction design parameters (see Ref. 7). Center column lists typical parameters when current biased in the quantum regime. Right column lists estimates of experimental time-scales.

$A=100\ \mu\text{m}^2$	$\omega_p/2\pi\approx 6$ GHz	$\omega_{10}t\sim 10^6$
$I_0=20\ \mu$A	$\Delta U/\hbar\omega_p\approx 4$	$f_m t\sim 10^{-6}$
$C=6$ pF	$\hbar\omega_p/kT\approx 15$	
$T=20$ mK		

on the transition direction, the spectral density $S_I^+(\omega/2\pi)$ is used in Eq. (10c) to find the phase noise

$$\langle\phi_n^2(t)\rangle=\left(\frac{\partial\omega_{10}}{\partial I_{dc}}\right)^2\int_0^{\omega_{10}/2\pi}df\,S_I^+(f)W_0(f). \tag{25}$$

Environmental and spin-boson calculations have previously calculated the effects of dissipation on decoherence.[9,2,8,10] In the Appendix we show that this calculation for the phase noise gives equivalent results.

We consider the case of a resistor environment $Y=1/R$. The decay rate of the $|1\rangle$ state is $\gamma_1=1/RC$. The phase noise is calculated from Eq. (25) to be

$$\langle\phi_n^2(t)\rangle\simeq\frac{kT}{3\Delta U}\frac{t}{RC}+\frac{\hbar\omega_p}{3\pi\Delta U}\frac{\ln(1.788\omega_{10}t)}{\omega_pRC}, \tag{26}$$

where we have used the formulas for $\omega_p(I)$ and $\Delta U(I)$ to find

$$(\partial\omega_{10}/\partial I_{dc})^2\simeq(\partial\omega_p/\partial I_{dc})^2 \tag{27a}$$

$$=1/6C\Delta U. \tag{27b}$$

The first term in $\langle\phi_n^2\rangle$ comes from thermal noise. Being proportional to time, it gives a phase decoherence rate $\gamma_\phi^{\text{th}}=(kT/6\Delta U)/RC$ for a Ramsey fringe experiment that is slower than the energy decay rate $1/RC$. The second term $\langle\phi_n^2\rangle^{\text{ZP}}$ comes from the zero-point noise, and varies in time only logarithmically. Because $\langle\phi_n^2\rangle^{\text{ZP}}$ is not proportional to t, describing it with a *rate* would be misleading. Instead, this term produces an error probability p_e for Ramsey fringes that is approximately constant over time. Using Eq. (15b), we calculate for $\langle\phi_n^2\rangle=\langle\phi_n^2\rangle^{\text{ZP}}$ and small errors

$$p_e=1-p_0 \tag{28a}$$

$$\simeq\langle\phi_n^2\rangle/4. \tag{28b}$$

For the typical junction parameters listed in Table I, we find the decoherence rates from energy decay and thermal phase noise are $\gamma_1=1/RC$ and $\gamma_\phi^{\text{th}}\simeq 1/360RC$, respectively. Decoherence is clearly dominated by the energy decay rate γ_1. For a junction capacitance of 6 pF, a coherence time of 10 μs requires $R=1.7\ \text{M}\Omega$. This magnitude of impedance can be achieved using broadband inductive impedance transformers.[7] For these parameters, the phase noise from zero-point fluctuations gives a error probability $p_e\simeq 0.1/\omega_pRC\sim 10^{-6}$ and thus is negligible.

When considering how noise causes decoherence, it is useful to categorize the noise for three frequency bands. At low frequencies less than $1/t\sim 10$ MHz, decoherence arises from phase noise produced by thermal and external noise. At intermediate frequencies $1/t$ to $\omega_{10}/2\pi$, phase decoherence is much less sensitive to noise because $W_0\propto 1/f^2$. Decoherence from quantum fluctuations is typically negligible unless for some frequency range the damping is not small and $\text{Re}Y/\omega_pC\gtrsim 0.01$. Finally, at the transition frequency ω_{10}, decoherence arises from spontaneous decay, and stimulated emission and absorption.

V. DECOHERENCE FROM A RESONANT CIRCUIT

The procedures presented in the previous section can be used to calculate decoherence for an arbitrary admittance. Because the important characteristics of the admittance are often resonances, we calculate in this section the effect of such resonances on decoherence. These results help the designer to understand the requirements of $Y(\omega)$ for good qubit operation. We consider the case of a single resonance mode with resonance frequency far from ω_{10}. For multiple resonances, the phase noise is summed from the results of the individual modes.

A series resonant circuit has an admittance $Y(\omega)=1/(R_s+i\omega L_s+1/i\omega C_s)$, where R_s, L_s, and C_s is the resistance, inductance, and capacitance of the circuit. For a low frequency resonance $\omega_s=1/\sqrt{L_sC_s}\ll\omega_{10}$ and low damping $R_s\ll\omega_sL_s$, we calculate from Eq. (25)

$$\langle\phi_n^2\rangle\simeq\left(\frac{\partial\omega_{10}}{\partial I_{dc}}\right)^2\langle I_n^2\rangle\frac{1-\cos(\omega_st)\exp(-tR_s/2L_s)}{2(\omega_s/2)^2}, \tag{29}$$

where $\langle I_n^2\rangle$ is the total noise in the resonant mode given by

$$\frac{1}{2}L_s\langle I_n^2\rangle=\frac{1}{4}\hbar\omega_s\text{cotanh}(\hbar\omega_s/2kT) \tag{30a}$$

$$=\frac{1}{2}kT\qquad(\hbar\omega\ll kT). \tag{30b}$$

The phase noise grows as $\langle\phi_n^2\rangle\simeq(\partial\omega_{10}/\partial I_{dc})^2\langle I_n^2\rangle t^2$ for times less than the oscillation period of the resonance $t<1/\omega_s$. With the amplitude of the phase noise proportional to t, the fluctuations can be understood as a change in the resonance frequency $(\partial\omega_{10}/\partial I_{dc})\langle I_n^2\rangle^{1/2}$ by the noise of the bias current.

For time $t\gg 1/\omega_s$, the phase noise does not grow larger because the change of the frequency is averaged over the oscillating noise. The magnitude of the phase noise may be estimated by ignoring the $\cos(\omega_st)$ term, and using $\omega_p\simeq\omega_{10}$ can be rewritten as

$$\langle\phi_n^2\rangle\simeq\frac{1}{6}\frac{\hbar\omega_{10}}{\Delta U}\frac{\omega_{10}L_J}{\omega_sL_s}\text{cotanh}(\hbar\omega_s/2kT). \tag{31}$$

A constant phase noise implies a constant measurement error. Using Eq. (28b), its magnitude is $p_e\sim 10^{-5}(\omega_{10}/\omega_s)$ for typical experimental parameters and realistic values of L_s

such that $L_s/L_J \simeq 100$. Although small, this measurement error may become significant if the resonant frequency is considerably below ω_{10} or if there are many low-frequency resonant modes.

For a high frequency resonance $\omega_s > \omega_{10}$, the current flowing through the junction is only a fraction $(\omega_{10}/\omega_s)^2$ of the total noise current. When combined with Eq. (31) and assuming $kT \ll \hbar\omega_{10}$, we find $p_e \simeq (\hbar\omega_{10}/24\Delta U)(Lj/L_s)(\omega_{10}/\omega_s)^5$. Because this result falls to zero rapidly with increasing resonance frequency, we conclude that resonances higher than ω_{10} produce negligible decoherence. This result justifies the use of $\omega_{10}/2\pi$ as the cutoff frequency in Eq. (25). For the case $\omega_s \simeq \omega_{10}$, the effect of the resonant mode must be solved with a full quantum mechanical calculation.

VI. DECOHERENCE FROM 1/*f* NOISE AND SPIN-ECHO SEQUENCES

Because actual experimental circuits have $1/f$ noise that at low frequencies far exceed the thermodynamic noise considered in Sec. IV , understanding and predicting this decoherence is crucial in order to optimally design Josephson qubits. We first consider $1/f$ charge noise, which should produce small phase noise but potentially gives significant amounts of decoherence from stimulated emission and absorption. We next consider critical current and flux $1/f$ noise, which produces phase noise. We calculate that the phase noise for spin-echo and Rabi sequences is much less than for the Ramsey sequence studied previously. Finally, we numerically estimate decoherence from $1/f$ noise using magnitudes of the noise obtained in the literature. Although $1/f$ noise is potentially the dominant source of decoherence, we argue that its effect can be made negligible by using spin-echo types of sequences.

Experiments on single-electron-tunneling devices have shown that tunnel junctions produce $1/f$ charge noise[20] with a spectral density $S_q(f) \simeq S_q^*(1\ \mathrm{Hz})/f$. The magnitude of this noise typically is $S_q^*(1\ \mathrm{Hz}) \simeq (10^{-3}e)^2$ for a junction with area $0.01\ \mu\mathrm{m}^2$. The spectral density of the noise scales as the area of the junction because the size of a junction is much larger than the characteristic distance of the charge fluctuations, typically an atomic dimension, causing the fluctuations to add incoherently.

The qubit considered here is sensitive to current noise, which is related to the charge noise by $S_I^q(f) = (2\pi f)^2 S_q(f) = (2\pi)^2 f S_q^*(1\ \mathrm{Hz})$. With spectral density proportional to *f*, Eq. (26) is used to calculate phase noise. This integral should have a cutoff frequency $\sim kT/h$ if the charge fluctuators are in thermal equilibrium. However, because experiments are consistent with $1/f$ charge noise that extends to frequencies as high as $\omega_{10}/2\pi$,[21] we calculate the phase noise as

$$\langle \phi_n^2 \rangle = \left(\frac{\partial\omega_{10}}{\partial I_{dc}}\right)^2 \int_0^{\omega_{10}/2\pi} df (2\pi)^2 f S_q^*(1\ \mathrm{Hz}) W_0(f) \quad (32a)$$

$$\simeq \frac{S_q^*(1\ \mathrm{Hz})/C}{\Delta U}\frac{2}{3}\ln(1.788\omega_{10}t). \quad (32b)$$

We find that this phase noise produces a negligible measurement error $p_e \simeq 5\times 10^{-6}$ for the experimental parameters previously listed.

Charge noise at frequency ω_{10} also produces stimulated emission and absorption at a rate calculated from Eq. (16) to be $\gamma_s = 2\pi^2 S_q^*(1\ \mathrm{Hz})/Ch$. We estimate $\gamma_s \sim (0.7\ \mu\mathrm{s})^{-1}$ using the measured noise spectral density at 1 Hz. Because this calculation assumes noise is present at frequencies $f \gg kT/h$ and extrapolates the $1/f$ noise power over 10 orders of magnitude in frequency, this rate is only a rough estimate and must be experimentally measured.

Phase noise also arises from critical-current and flux $1/f$ fluctuations. These noise sources produce an effective current noise $S_I^{1/f} = S_{I_0} + S_\Phi/L^2$ for our circuit, where S_{I_0} and S_Φ are the experimentally determined spectral density of the critical current and flux noise, respectively, and L is the inductance of the loop connected to the qubit junction. For a noise spectral density $S_I^{1/f}(f) = S_I^*(1\ \mathrm{Hz})/f$, the phase noise is

$$\langle \phi_n^2(t) \rangle = \left(\frac{\partial\omega_{10}}{\partial I_{dc}}\right)^2 \int_{f_m}^{\omega_{10}/2\pi} df \frac{S_I^*(1\ \mathrm{Hz})}{f} W_0(f) \quad (33a)$$

$$\simeq \left(\frac{\partial\omega_{10}}{\partial I_{dc}}\right)^2 S_I^*(1\ \ \mathrm{Hz})\ln(0.401/f_m t)t^2 \quad (33b)$$

$$= \frac{S_I^*(1\ \ \mathrm{Hz})L_J}{\Delta U}\frac{\ln(0.401/f_m t)}{6}(\omega_{10}t)^2, \quad (33c)$$

where f_m corresponds to the frequency of the entire measurement and gives a low-frequency cutoff. Apart from the slowly varying logarithm term, the phase noise is found to be proportional to t^2 and thus can not be understood as a rate. Instead, it is better understood as a change in oscillation frequency for every repetition of an experiment.

Decoherence from phase noise can be reduced[4] by operating the qubit so that drifts in the oscillation frequency are cancelled out. The method is analogous to spin echo in nuclear magnetic resonance, or lock-in techniques that are commonly used to reduce the effect of $1/f$ noise.

For spin echo, the sequence of control pulses are $\vec{c}_0 = (0,\pi/2,0)$, wait for time $t/2$, $\vec{c}_1 = (0,\pi,0)$, wait for time $t/2$, then $\vec{c}_2 = (0,\pi/2,0)$. This is similar to the Ramsey fringe sequence except for an additional control pulse at time $t/2$ that interchanges the states $|0\rangle$ and $|1\rangle$, thus reversing the low-frequency drift. The phase noise for this sequence is

$$\phi_n(t) = \frac{\partial\omega_{10}}{\partial I_{dc}}\left(\int_0^{t/2} dt' I_n(t') - \int_{t/2}^{t} dt' I_n(t')\right). \quad (34)$$

The mean squared amplitude of the phase noise may be found using Eq. (10c), but with a spectral weight for the spin echo sequence given by

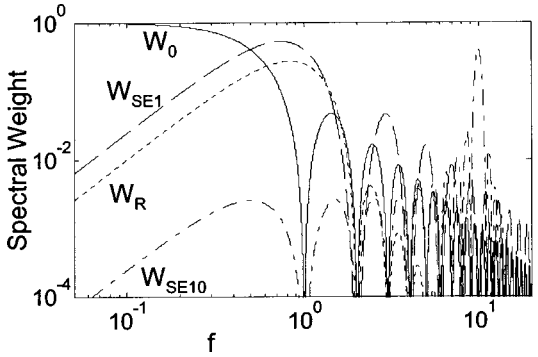

FIG. 3. Spectral weight functions vs frequency f, plotted for $t=1$ and four control sequences described in text: Ramsey W_0, $N=1$ spin echo W_{SE1}, Rabi W_R, and $N=10$ spin echo W_{SE10}.

$$W_{\mathrm{SE1}}(f)=\left|\int_0^{t/2}dt'e^{i2\pi ft'}-\int_{t/2}^{t}dt'e^{i2\pi ft'}\right|^2 \tag{35a}$$

$$=\tan^2(\pi ft/2)\frac{\sin^2(\pi ft)}{(\pi f)^2}. \tag{35b}$$

Comparing this result with $W_0(f)$, we find that the additional term $\tan^2(\pi ft/2)$ renders the phase noise insensitive to low frequency noise. We calculate for a generalization of the spin echo experiment using $2N-1$ π pulses

$$W_{\mathrm{SEN}}(f)=\tan^2(\pi ft/2N)\frac{\sin^2(\pi ft)}{(\pi f)^2}, \tag{36}$$

where t is the time between the two $\pi/2$ Ramsey pulses. In Fig. 3 we plot the spectral weight function for the case of no spin echo as well as with spin echo for $N=1$ and $N=10$. This figure shows that the spectral weight functions for spin echo are no longer sensitive to noise at dc and very low frequencies, but are mainly sensitive to noise at the frequency $f_r=N/t$.

Rabi oscillations are also insensitive to low-frequency noise. They are observed with a pulse sequence consisting of a microwave pulse of frequency ω_{10} and duration t with an amplitude such that $\vec{c}=(0,2\pi N,0)$. The calculation proceeds similarly as for spin echo except that the noise moves the Bloch vector out of the $\hat{x}$-$\hat{y}$ plane, and ϕ_n now represents the magnitude of the Bloch vector in the $\hat{y}$ direction. The prediction for phase noise is similar to previous results but has a spectral weight function

$$W_{\mathrm{R}}(f)=\left|\int_0^{t}dt'e^{i2\pi ft'}\sin(2\pi f_r t')\right|^2 \tag{37a}$$

$$=\left(\frac{f_r f}{f_r^2-f^2}\right)^2\frac{\sin^2(\pi ft)}{(\pi f)^2}. \tag{37b}$$

This spectral weight function has a shape comparable to the spin-echo function, but has smaller harmonic weight.

Decoherence for the Ramsey, spin-echo, and Rabi pulse sequences may be evaluated and compared for white and $1/f$ noise. For constant spectral density S_I^0, the Ramsey and spin echo sequences both give $\langle\phi_n^2(t)\rangle=(\partial\omega_{10}/\partial I_{dc})^2S_I^0t/2$. The Rabi sequence gives a result 1/2 as large because the low-frequency noise affects the Bloch vector less during the time the vector points in the $\hat{z}$ direction. For $1/f$ noise, because the spectral-weight function peaks at frequency $f_r=N/t$, the phase noise is well approximated by

$$\langle\phi_n^2(t)\rangle_a=(\partial\omega_{10}/\partial I_{dc})^2S_I(f_r)t/2 \tag{38}$$

for the spin-echo sequence, and 1/2 this expression for the Rabi sequence. This expression is identical to the results for white noise but with the noise spectral density being evaluated at frequency f_r. This result agrees well with that obtained from numerical integration, as shown in Table II. Note that the phase noise is slightly larger than the approximate result for the Rabi sequence because of the decreased harmonic content in the spectral weight function. Because the phase noise $\langle\phi_n^2(t)\rangle_a$ increases linearly with time, the decoherence can now be described with a rate.

TABLE II. Table of $\langle\phi_n^2(t)\rangle/\langle\phi_n^2(t)\rangle_a$ for six values of N, numerically calculated for $1/f$ noise, and the spin echo and Rabi pulse sequences. Numerical values close to one confirm Eq. (38) is a good approximation.

N	**1**	**2**	**3**	**5**	**10**	**100**
SpinEcho	1.386	1.204	1.121	1.040	0.962	0.869
Rabi	1.397	1.266	1.204	1.143	1.085	1.013

When the noise spectral density is $1/f$, spin echo or Rabi sequences significantly reduce decoherence as compared to a Ramsey sequence. In contrast, there is no difference between the sequences when the noise is white because the noise is uncorrelated in time. Comparing Eq. (38) with Eq. (33c), we find the phase noise is lowered with spin echo by a factor $2N\ln(0.401/f_mt)$, which is a large factor $\sim$26 even for $N=1$.

We use Eq. (38) to estimate the coherence time of a quantum computer under the assumption that the operation of the computer will incorporate pulse sequences that interchanges the qubit states in order to reduce the effect of low-frequency noise. Additionally, since the spectral weight functions peaks at the frequency $f_r=N/t$, the frequency dependence of the noise spectral density can be measured with the spin echo and Rabi pulse sequences. This experiment would verify if the dominant decoherence mechanism is $1/f$ noise and measure its magnitude.

In Table III we list our estimates for the phase decoherence rates from published values of the $1/f$ noise. Experiments have shown that the critical-current noise[22] has S_{I_0}

TABLE III. Table of phase noise and decoherence rates for two types of 1/f noise. Scaling with junction area A is also listed. A spin echo frequency of 10^7Hz has been assumed.

$1/f$ noise	Ramsey $\langle\phi_n^2(t)\rangle$	Spin echo, γ_ϕ	Scaling
I_0	$(t/14\ \mu\mathrm{s})^2$	$(48\ \mathrm{ms})^{-1}$	$A^{2/3}$
Φ	$(t/50\ \mu\mathrm{s})^2$	$(620\ \mathrm{ms})^{-1}$	A^{-1}

$\simeq S^*_{I_0}(1\ \mathrm{Hz})/f$, with $S^*_{I_0}(1\ \mathrm{Hz}) \simeq (10^{-6} I_0)^2$ for a 100 $\mu\mathrm{m}^2$ area junction at 4 K. The parameter $S^*_{I_0}(1\ \mathrm{Hz})/I_0^2$ has been found[23] to scale inversely with junction area and proportional to T^2 down to at least 100 mK. We estimate for the junction parameters of Table I a noise $S_I(f) = (10^{-6} I_0)^2 (0.1\ \mathrm{K}/4\ \mathrm{K})^2/f$. Equation (33c) predicts for a Ramsey fringe experiment $\langle \phi_n^2(t) \rangle \sim (t/14\ \mu\mathrm{s})^2$, whereas Eq. (38) gives for a spin-echo sequence with frequency 10^7 Hz a decoherence rate $\gamma_\phi = (48\ \mathrm{ms})^{-1}$. Measurements on flux noise has shown $S_\Phi \simeq S^*_\Phi(1\ \mathrm{Hz})/f$, where $S^*_\Phi(1\ \mathrm{Hz}) \simeq (5 \times 10^{-6} \Phi_0)^2$ does not vary greatly with inductor value or temperature.[24,25,23] Flux noise[26–28] gives for $L = 3$ nH a spectral current density $S_I(f) = (5 \times 10^{-6} \Phi_0)^2/(3\ \mathrm{nH})^2 f$. We predict for a Ramsey fringe experiment $\langle \phi_n^2(t) \rangle \sim (t/50\ \mu\mathrm{s})^2$, whereas we find $\gamma_\phi = (620\ \mathrm{ms})^{-1}$ for a spin-echo sequence with frequency 10^7 Hz. These estimations indicate that $1/f$ noise should not be a significant limitation for coherence if logic operations use spin-echo type sequences.

We can also estimate how decoherence changes with junction area A. The junction parameters should be scaled as $C \propto A$ and $I_0 \propto A^{2/3}$ if we use the condition that ΔU and ω_p are held constant with changes in A. This implies that the critical-current density of the junction scales as $1/A^{1/3}$. As discussed previously, the decay rate due to dissipation of the environment is $\gamma_1 = \mathrm{Re}\, Y(\omega_{10})/C$. Because the impedance transformation of $\mathrm{Re}\, Y$ is inversely proportional to the square of the critical current of the filter junction[7] and its critical-current scales with the qubit area, we find $\gamma_1 \propto 1/A^{7/3}$. The decoherence from charge noise is $S^*_q(1\ \mathrm{Hz})/C$, which implies that there is no dependence on area. For critical current noise, the decoherence scales as $S^*_{I_0}(1\ \mathrm{Hz})/C \propto A^{2/3}$. Because flux noise is independent of junction parameters, its decoherence is proportional to $1/A$. Since decoherence can either increase or decrease with area depending on the mechanism, its proper optimization depends on the exact numerical values of the circuit, its impedance transformer, and noise sources. The present junction parameters can be further optimized after we experimental measure and confirm how these noise mechanisms affect decoherence.

VII. DECOHERENCE FROM NON-GAUSSIAN NOISE

Decoherence calculations typically assume a Gaussian distribution of the noise. Because this assumption may not be obeyed for $1/f$ noise in Josephson junctions, we present in this section a qualitative analysis that may be useful for interpreting experiments. A non-Gaussian source can affect a Ramsey fringe experiment in a way that is qualitatively different than described earlier in Sec. III.

Noise sources are typically well described by Gaussian statistics because the noise is averaged over a large number of fluctuators. However, individual fluctuators can be observed in Josephson junctions, particularly submicrometer area devices.[25,20] A single fluctuator can produce sudden and large changes in the noise signal at random times, and is often described as ''random telegraph noise.'' For simplicity, we consider the case of a single random-telegraph fluctuator superimposed on a noise background that is Gaussian and white.

If a Ramsey experiment is performed during the time when the telegraph noise is not active, then the state evolves in the normal way. An average over such events gives the usual decay of the state probability. But if the experiment overlaps with a telegraph fluctuation, then the fluctuation adds noise to the phase. For simplicity, if we assume large random telegraph fluctuations, the phase noise becomes large enough to randomize the individual state measurements. When both the Gaussian and telegraph events are averaged together, we expect a measurement of the Ramsey fringes to give the usual state decay but with reduced amplitude.

This reduction in magnitude is an interesting prediction because it can mimic loss of fidelity from the state measurement. These two mechanisms probably can be distinguished only with careful experiments.

VIII. SUMMARY AND CONCLUSIONS

We have calculated the effective two-state Hamiltonian for the current-biased Josephson junction, and have shown that a qubit state can be fully manipulated with the control currents. Noise in the control currents produces decoherence in the qubit, with noise at microwave frequencies affecting the relative population between the ground and excited state, and noise at low frequency affecting the phase of the state. The finite impedance of the current bias produces decoherence in a manner that can be calculated semiclassically by appropriately adding thermal and zero-point noise.

There are several advantages to calculating decoherence with noise. Noise calculations give a physical understanding to the origins of decoherence, and may be easily extended to include arbitrary admittance, noise spectral density, manipulation sequences, and noise statistics. Because decoherence depends on a measurement sequence, a precise representation of decoherence must describe fluctuations in the rotations ϕ, θ_x, and θ_y.

Decoherence from spin echo and Rabi sequences is much less sensitive to low frequency noise than Ramsey sequences. We have derived an approximate decoherence rate that shows for spin-echo sequences the appropriate noise spectral density is evaluated at the manipulation frequency. We estimated decoherence rates for the current-biased Josephson junction systems using experimental values of charge, critical current, and flux $1/f$ noise. These rates indicate that this system is a good candidate for a solid-state quantum computer.

An increase in coherence motivates the use of spin-echo type sequences for logic operations in a quantum computer. These sequences may also be used to directly measure the noise spectral density in these qubits.

Noise theory calculates decoherence in a clear and physical manner, and is especially useful in superconducting systems because there is much experience understanding and predicting the noise performance of devices with noise models. We hope that this approach will be used to better

understand and predict decoherence in other superconducting qubits, as well as for other solid-state qubit systems.

ACKNOWLEDGMENTS

We thank J. Clarke, R. Schoelkopf, D. Esteve, and M. Devoret for helpful discussions. This work was supported in part by the NSA under Contract No. MOD709001.

APPENDIX: ENVIRONMENTAL CALCULATION OF THE PHASE NOISE

We compare here our results for phase noise with previous calculations based on standard quantum calculations of the environment and spin-boson models. We are mostly concerned with comparing the form of the phase-noise integral and checking that quantum noise is included properly. Calculations for the Cooper-pair box system give slightly different formulas for the phase fluctuations since they are sensitive to voltage fluctuations from the environment.

As in Sec. III, dephasing from the environment is calculated from the correlator $\langle e^{i[\phi(t)-\phi(0)]}\rangle$, where $\phi(t)$ is given by Eq. (8). For Gaussian noise we have

$$\langle e^{i[\phi(t)-\phi(0)]}\rangle = e^{\langle[\phi(t)-\phi(0)]\phi(0)\rangle} \equiv e^{J(t)}.$$

Note that $J(t)$ is calculated exactly as for the $P(E)$ theory of the environment,[29] and the real part of J corresponds to phase fluctuations. From the environmental theory [see Eqs. (1) and (2) of Ref. 10), we find

$$\mathrm{Re}\{J(t)\} = -4\int_0^\infty \frac{d\omega}{\omega}\,\frac{\mathrm{Re}\,Z_t(\omega)}{R_K}\coth\left(\frac{\hbar\omega}{2kT}\right)[1-\cos(\omega t)]. \tag{A1}$$

This equation can be rewritten as

$$\mathrm{Re}\{J(t)\} = -\left(\frac{e}{\hbar}\right)^2\int_0^\infty \frac{d\omega}{2\pi}S_V^+(\omega/2\pi)\,\frac{\sin(\omega t/2)}{(\omega/2)^2}, \tag{A2}$$

where the voltage spectral density is

$$S_V^+(\omega/2\pi) = 2\hbar\omega\,\mathrm{Re}\,Z_t(\omega)\,\mathrm{cotanh}\left(\frac{\hbar\omega}{2kT}\right). \tag{A3}$$

This result is identical in form to Eq. (25). Equation (4.17) of Ref. 2 gives the same corresponding integral for the phase noise.

*Electronic address: martinis@boulder.nist.gov

†Electronic address: urbina@cea.fr

[1] M. A. Nielsen and I. L. Chuang, *Quantum Computation and Quantum Information* (Cambridge University Press, Cambridge, 2000).

[2] Y. Makhlin, G. Schön, and A. Shnirman, Rev. Mod. Phys. **73**, 357 (2001).

[3] Y. Nakamura, C. D. Chen, and J. S. Tsai, Phys. Rev. Lett. **79**, 2328 (1997).

[4] Y. Nakamura, Y. A. Pashkin, T. Yamamoto, and J. S. Tsai, Phys. Rev. Lett. **88**, 047901 (2002).

[5] D. Vion, A. Aassime, A. Cottet, P. Joyez, H. Pothier, C. Urbina, D. Esteve, and M. H. Devoret, Science **296**, 886 (2002).

[6] S. Han, Y. Yu, Xi Chu, S. Chu, and Z. Wang, Science **293**, 1457 (2001). Y. Yu, S. Han, X. Chu, S. Chu, and Z. Wang, *ibid.* **296**, 889 (2002).

[7] J. M. Martinis, S. Nam, J. Aumentado, and C. Urbina, Phys. Rev. Lett. **89**, 117901 (2002).

[8] A. Shnirman, Y. Makhlin, and G. Schon, Phys. Scr. (to be published).

[9] A. Cottet, A. Steinbach, P. Joyez, D. Vion, H. Pothier, D. Esteve, and M.E. Huber (unpublished).

[10] J.P. Pekola and J.J. Toppari, Phys. Rev. B **64**, 172509 (2001).

[11] L. Tian, S. Lloyd, and T. P. Orlando, Phys. Rev. B **65**, 144516 (2002).

[12] A. J. Leggett, *Chance and Matter*, edited by J. Souletie, J. Vannimenus, and R. Stora (Elsevier, Amsterdam, 1987), 395.

[13] J. M. Martinis, M. H. Devoret, and J. Clarke, Phys. Rev. B **35**, 4682 (1987).

[14] J. Clarke, A. N. Cleland, M. H. Devoret, D. Esteve, and J. M. Martinis, Science **239**, 992 (1988).

[15] J. M. Martinis, M. H. Devoret, and J. Clarke, Phys. Rev. Lett. **55**, 1543 (1985).

[16] Equation (15b) is correct to lowest order in $\langle\theta_x^2\rangle$ and $\langle\theta_y^2\rangle$. It is exact if $\langle\theta_x^2\rangle = 0$ or $\langle\theta_y^2\rangle = 0$.

[17] M. H. Devoret, in *Fluctuations Quantiques* (Elsevier, Science, 1997).

[18] This noise model also makes the implicit assumption of weak coupling to many environmental modes. For the case of strong coupling and $1/f$ noise, see E. Paladino, L. Faoro, G. Falci, and R. Fazio, Phys. Rev. Lett. **88**, 228304 (2002).

[19] D. Esteve, M. H. Devoret, and J. M. Martinis, Phys. Rev. B **34**, 158 (1986).

[20] G. Zimmerli, T. M. Eiles, R. L. Kautz, and J. M. Martinis, Appl. Phys. Lett. **61**, 237 (1992); J. Ahlers, J. Niemeyer, T. Weimann, H. Wolf, V. A. Krupenin, and S. V. Lotkhov, Phys. Rev. B **53**, 13 682 (1996).

[21] M. Covington, M. Keller, R. Kautz, and J. M. Martinis, Phys. Rev. Lett. **84**, 5192 (2000).

[22] B. Savo, F. Wellstood, and J. Clarke, Appl. Phys. Lett. **50**, 1757 (1987).

[23] F. Wellstood, Ph.D. thesis, U.C. Berkeley, 1988.

[24] R. Koch, J. Clarke, W. Goubau, J. Martinis, C. Pegrum, and D. VanHarlingen, J. Low Temp. Phys. **51**, 207 (1983).

[25] F. C. Wellstood, C. Urbina, and J. Clarke, Appl. Phys. Lett. **50**, 772 (1987).

[26] Flux-noise has been measured for devices at low temperature in a manner where vortices are probably trapped in the superconducting film (Ref. 27). In high-T_c devices, when vortices were eliminated through careful film design and low-field cooling, flux noise was greatly reduced (Ref. 28). This noise reduction has yet to be demonstrated for low-T_c devices.

[27] G. Stan, S. Field, and J. M. Martinis (unpublished).

[28] E. Dantsker, S. Tanaka, and J. Clarke, Appl. Phys. Lett. **70**, 2037 (1997).

[29] M. H. Devoret, D. Esteve, H. Grabert, G. L. Ingold, and H. Pothier, Phys. Rev. Lett. **64**, 1824 (1990).